Thermo-Mechanical Analysis of Industrial Solidification Processes

M. Cervera
C. Agelet de Saracibar
M. Chiumenti

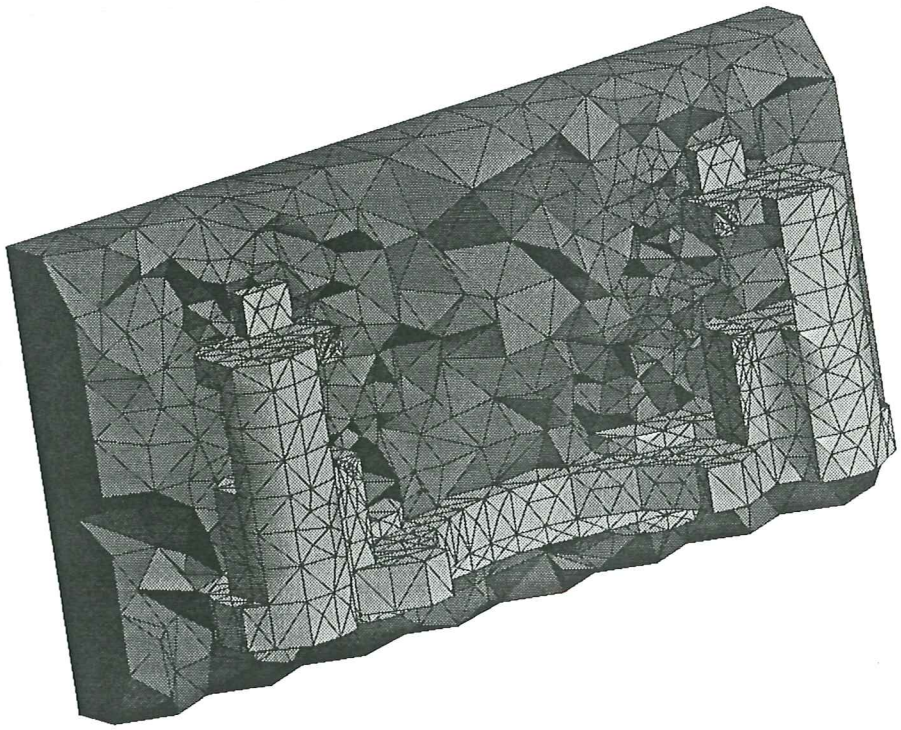

Publication CIMNE Nº 153, January 1999

Thermo-Mechanical Analysis of Industrial Solidification Processes

M. Cervera
C. Agelet de Saracibar
M. Chiumenti

Publication CIMNE Nº 153, January 1999

International Center for Numerical Methods in Engineering
Gran Capitán s/n, 08034 Barcelona, Spain

THERMO-MECHANICAL ANALYSIS OF INDUSTRIAL SOLIDIFICATION PROCESSES

Miguel Cervera, Carlos Agelet de Saracibar and Michele Chiumenti

International Center for Numerical Methods in Engineering (CIMNE)
Universidad Politécnica de Cataluña
Campus Norte UPC, 08034 Barcelona, Spain
e-mail: cervera@cimne.upc.es, web page: http://cimne.upc.es/

Key words: Thermo-mechanical Analysis, Solidification Processes, Coupled Solution.

Abstract. *The paper presents an up-to-date finite element numerical model for fully coupled thermo-mechanical problems, focussing in the simulation of solidification processes of industrial metal parts. The proposed constitutive model is defined by a thermo-visco-elasto-(visco)plastic free energy function which includes a contribution for thermal multiphase changes. Mechanical and thermal properties are assumed to be temperature dependent, and viscous-like strains are introduced to account for the variation of the elastic moduli during the cooling process. The continuous transition between the initial fluid-like and the final solid-like behaviour of the part is modelled by considering separate viscous and elasto-plastic responses as a function of the solid fraction. Thermo-mechanical contact conditions between the mould and the part are specifically considered, assuming that the heat flux is a function of the normal pressure and the thermal and mechanical gaps. A fractional step method arising from an operator split of the governing equations is used to solve the nonlinear coupled system of equations, leading to a staggered product formula solution algorithm suitable for large scale computations. Representative simulations of industrial solidification processes are shown, and comparison of computed results using the proposed model with available experimental data is given.*

1 INTRODUCTION

The numerical simulation of coupled thermo-mechanical solidification processes has been one of the research topics of great interest over the last years. Also, during the last decade, a growing interest on this and related topics has been shown by many industrial companies, such as automotive and aeronautical, motivated by the need to get high quality final products and to reduce manufacturing costs. However, and despite the enormous progress achieved lately in computational mechanics, the large scale numerical simulation of these problems continues to be nowadays a very complex task. This is mainly due to the highly nonlinear nature of the problem, usually involving nonlinear constitutive behaviour, liquid-solid and solid-solid phase changes, nonlinear thermal and mechanical boundary conditions, frictional contact interaction and complex coupled thermo-mechanical phenomena. In this paper the topic of the numerical simulation of industrial solidification processes is addressed.

2 FORMULATION OF THE THERMO-MECHANICAL PROBLEM

2.1 Local Governing Equations

The local system of partial differential equations governing the (quasi-static) coupled thermo-mechanical initial boundary value problem is defined by the momentum and energy balance equations, restricted by the inequalities arising from the second law of the thermodynamics. The local form of the momentum and energy balance equations can be written as

$$\begin{aligned} 0 = &\quad \nabla \cdot \boldsymbol{\sigma} + \boldsymbol{B} \\ \Theta \dot{S} = &-\nabla \cdot \boldsymbol{q} + R + \mathcal{D}_{int} \end{aligned} \tag{1}$$

where $\boldsymbol{B}$ are the (prescribed) body forces, $\nabla \cdot (\cdot)$ the divergence operator, $\boldsymbol{\sigma}$ the Cauchy stress tensor, Θ the absolute temperature, S the entropy, $\boldsymbol{q}$ the heat flux, R the (prescribed) heat source and $\mathcal{D}_{int}$ the internal dissipation per unit volume. Additionaly, suitable prescribed boundary and initial conditions must be supplied, as well as considering the equilibrium equations at the contact interfaces.

Also, the entropy S and the Cauchy stress tensor $\boldsymbol{\sigma}$ must be defined via constitutive relations, subjected to the following restriction on the internal dissipation:[1]

$$\mathcal{D}_{int} = \boldsymbol{\sigma} : \dot{\boldsymbol{\epsilon}} + \Theta \dot{S} - \dot{E} \ \geq 0 \tag{2}$$

where $\boldsymbol{\epsilon}$ is the infinitesimal strain tensor and E is the internal energy. The heat flux $\boldsymbol{q}$ is related to the absolute temperature through Fourier's law ($\boldsymbol{q} = -k(\Theta)\ \nabla\Theta$, with $k = k(\Theta)$ being the temperature dependent thermal conductivity), subjected to the restriction on the dissipation by conduction:

$$\mathcal{D}_{con} = -\frac{1}{\Theta} \nabla\Theta \cdot \boldsymbol{q} = \frac{k(\Theta)}{\Theta} \nabla\Theta \cdot \nabla\Theta \ \geq 0 \tag{3}$$

The state equations are obtained from Eq. (4) using Coleman's method as:[1]

$$\begin{aligned} \boldsymbol{\sigma} = \quad \partial_{\boldsymbol{\epsilon}} \hat{\Psi} &= K(\Theta)\, e_e\, \mathbf{1} + 2\, G(\Theta)\, \mathrm{dev}\,[\boldsymbol{\epsilon}_e] \\ S = -\,\partial_{\Theta} \hat{\Psi} &= \int_{\Theta_0}^{\Theta} C_0(\hat{\Theta})\, \frac{d\hat{\Theta}}{\hat{\Theta}} \;-\; \partial_{\Theta} \hat{W} \;-\; \partial_{\Theta} \hat{H} \end{aligned} \tag{10}$$

where the term $-\partial_{\Theta}\hat{W} = 3K(e_e + e_{\Theta})[\alpha + \alpha_{\Theta}(\Theta_0 - \Theta_{ref})] - \frac{1}{2}K_{\Theta}(e_e^2 - e_{\Theta}^2)$ may be different from zero even if the material properties are constant.

The internal dissipation can be expressed in terms of the evolution of the internal variables as

$$\mathcal{D}_{int} = \boldsymbol{\sigma} : \dot{\boldsymbol{\epsilon}}_v + \boldsymbol{\sigma} : \dot{\boldsymbol{\epsilon}}_p + q\,\dot{\xi} \;\geq 0 \tag{11}$$

where q is the conjugate variable of ξ, that is, $q = -\partial_{\xi}\hat{\Psi} = -\partial_{\xi}\hat{H}$.

Note that considering the constitutive equation for the entropy and taking its time derivative and applying the chain rule the heat capacity and the elastoplastic heating can be defined as

$$\begin{aligned} C_s(\Theta) &:= \Theta\, \partial_{\Theta} S && = C_0(\Theta) \;-\; \Theta\, \partial^2_{\Theta\Theta}\,(\,\hat{W} \,+\, \hat{H}\,) \\ \mathcal{H}_{ep}(\Theta) &:= \Theta\,(\partial_{\boldsymbol{\epsilon}} S : (\dot{\boldsymbol{\epsilon}}_e + \dot{\boldsymbol{\epsilon}}_{\Theta}) + \partial_{\xi} S\, \dot{\xi}) = -\Theta\, \partial_{\Theta}\,(\boldsymbol{\sigma} : (\dot{\boldsymbol{\epsilon}}_e + \dot{\boldsymbol{\epsilon}}_{\Theta}) - q\,\dot{\xi}) \end{aligned} \tag{12}$$

where Eq. (5) and the equalities $\partial_{\boldsymbol{\epsilon}} S = -\partial_{\Theta}\boldsymbol{\sigma}$ and $\partial_{\xi} S = \partial_{\Theta} q$ have been used. With these definitions at hand, Eq. (1.b) can be rewritten in the usual temperature form as

$$C_s\,\dot{\Theta} = -\nabla \cdot \boldsymbol{q} + R + \mathcal{D}_{int} - \mathcal{H}_{ep} \tag{13}$$

In the case of an increase of the temperature-dependent elastic moduli due to the cooling process of a loaded elastic solid, irrecoverable strains necessarily occur. These strains are evident if a sample loaded with given elastic moduli is unloaded at a later time when the temperature has dropped and, therefore, the elastic moduli are higher. This stiffening effect is incorporated in the constitutive model introducing a viscous strain tensor as an internal variable. Taking the time derivative of Eq. (10.a) yields

$$\dot{\boldsymbol{\sigma}} \;=\; (K(\Theta)\,\dot{e}_e \;+\; \dot{K}(\Theta)\, e_e)\,\mathbf{1} \;+\; 2\,G(\Theta)\,\mathrm{dev}\,[\dot{\boldsymbol{\epsilon}}_e] \;+\; 2\,\dot{G}(\Theta)\,\mathrm{dev}\,[\boldsymbol{\epsilon}_e] \tag{14}$$

On the other hand, the experimental observation of the relation between the rate of stress and the rate of strain takes the form:

$$\begin{aligned} \dot{\boldsymbol{\sigma}} &= K(\Theta)\,(\dot{\epsilon} \;-\; \dot{\epsilon}_{\Theta})\,\mathbf{1} \;+\; 2\,G(\Theta)\,\mathrm{dev}\,[\,\dot{\boldsymbol{\epsilon}} \;-\; \dot{\boldsymbol{\epsilon}}_p\,] \\ &= K(\Theta)\,(\dot{e}_e \;+\; \dot{e}_v)\,\mathbf{1} \;+\; 2\,G(\Theta)\,\mathrm{dev}\,[\,\dot{\boldsymbol{\epsilon}}_e \;+\; \dot{\boldsymbol{\epsilon}}_v\,] \end{aligned} \tag{15}$$

Equating Eq. (14) to Eq. (15.a) yields the following evolution law for the viscous strain:

$$\dot{\boldsymbol{\epsilon}}_v \;:=\; \frac{\langle \dot{K} \rangle}{K}\, e_e\, \mathbf{1} \;+\; \frac{\langle \dot{G} \rangle}{G}\,\mathrm{dev}\,[\boldsymbol{\epsilon}_e] \;=\; \frac{\langle \dot{K} \rangle}{K^2}\, p\, \mathbf{1} \;+\; \frac{\langle \dot{G} \rangle}{2G^2}\,\mathrm{dev}\,[\boldsymbol{\sigma}] \tag{16}$$

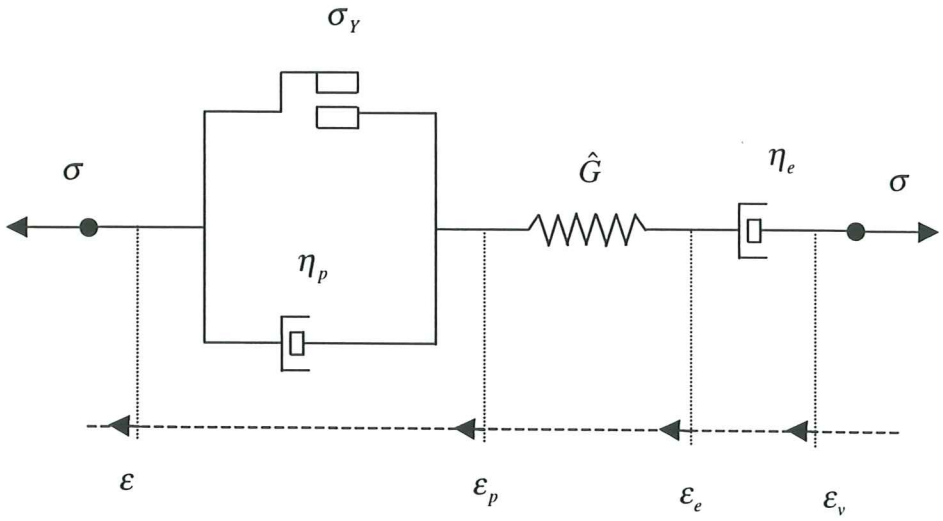

Figure 1. Rheological mechanical model with phase change.

where $\hat{G} = G(\Theta)/f_s(\Theta)$ is the effective (temperature dependent) shear modulus. The evolution law of the viscous strains, Eq. (16), is also modified to account for the viscous behaviour of the fluid, and it is rewritten as

$$\dot{\boldsymbol{\epsilon}}_v := \frac{\langle \dot{K} \rangle}{K^2} p\,\mathbf{1} + \Big(\frac{\langle \dot{\hat{G}} \rangle}{2\hat{G}^2} + \frac{1}{\hat{\eta}_e} \Big) \operatorname{dev}[\boldsymbol{\sigma}] \tag{21}$$

where the $\hat{\eta}_e = \eta_e(\Theta)/f_l(\Theta)$ is the effective (temperature dependent) elastic viscosity. Note that for the solid phase $f_l(\Theta) = 0$ and, therefore, $\hat{\eta}_e = \infty$, and the solid model is recovered. On the other hand, for the fluid phase $f_s(\Theta) = 0$ and, therefore, $\hat{G} = \infty$ and a pure Norton's model is recovered.

Also the volumetric change due to the phase change is included, so that Eq. (6) is rewritten as

$$\boldsymbol{\epsilon}_\Theta = [\,\alpha(\Theta)(\Theta - \Theta_{ref}) \;-\; \alpha(\Theta_0)(\Theta_0 - \Theta_{ref}) \;+\; \frac{1}{3}\, e_{pc}\,(f_s(\Theta) - f_s(\Theta_0))\,]\,\mathbf{1} \tag{22}$$

where e_{pc} is the volumetric variation due to phase change. Usually, this consists of a volumetric contraction referred to as phase change shrinkage ($e_{pc} < 0$).

Finally, the thermal term of the free energy $T = \hat{T}(\Theta)$ must be extended to account for the thermal effects of the phase change. In this work, it will take the form:

$$T = \hat{T}(\Theta) = \int_{\Theta_0}^{\Theta} \hat{T}_\Theta(\bar{\Theta})\, d\bar{\Theta} = -\int_{\Theta_0}^{\Theta} d\bar{\Theta} \int_{\Theta_0}^{\bar{\Theta}} [\,C_0(\hat{\Theta}) + L_\Theta(\hat{\Theta})\,] \frac{d\hat{\Theta}}{\hat{\Theta}} \tag{23}$$

where $L = L(\Theta)$ is the latent heat function. It is possible to define the latent heat function in terms of the solid fraction as $L = \mathcal{L}\, f_s(\Theta)$, with $\mathcal{L}$ constant, but there are

3 TIME INTEGRATION OF THE COUPLED PROBLEM

The numerical solution of the coupled thermomechanical IBVP involves the transformation of an infinite dimensional transient system, governed by a system of quasi-linear partial differential equations into a sequence of discrete nonlinear algebraic problems by means of a Galerkin finite element projection and a time marching scheme for the advancement of the primary nodal variables, displacements and temperatures, together with a return mapping algorithm for the advancement of the internal variables.

With regard to the time marching scheme different strategies are possible to perform this transformation, but they can be grouped in two categories: *simultaneous* time-stepping algorithms and *staggered* time-stepping algorithms.

Simultaneous time-stepping algorithms solve both the mechanical and the thermal equilibrium equations together, thus advancing all the primary nodal variables of the problem, displacements and temperatures, simultaneously. This invariably leads to large and unsymmetric systems of equations, usually prohibitively expensive to solve. Furthermore, the use of different standard time-stepping algorithms developed for the single uncoupled problems is not straightforward, and it is not possible to take advantage of the different time scales possibly involved in the problem for the mechanical and thermal parts. On the other hand, it is relatively simple to devise unconditionally stable schemes using this approach.

A variant of this approach is to attempt the solution of the resulting equations using a block-iterative solution. This leads to smaller and usually symmetric system of equations to be solved, but then the study of the stability of the algoriths is complicated, as it depends on the tolerances used to assess convergenge. The problem of stability in time is then linked to that of convergence within the time step.[11]

Staggered time-stepping algorithms are based on the use of an operator split, applied to the coupled system of nonlinear ordinary differential equations, and a product formula algorithm, which leads to a scheme in which each one of the subproblems defined by the partition is solved sequentially, within the framework of classical *fractional step methods.* This leads to the partition of the original problem into smaller and typically symmetric (physical) subproblems. Furthermore, the use of different standard time-stepping algorithms developed for the uncoupled subproblems is now straightforward, and it is possible to take advantage of the different time scales involved. Additionally, it is now possible to obtain unconditionally stable schemes using this approach, providing that the operator split preserves the underlying dissipative structure of the original problem[12,13]. In view of these motivations, in this work the staggered scheme has been preferred. Additional details about the formulation, implementation and stability analysis of the method can be found in references 2, 3, 12 and 13.

In the classical *isothermal split* the coupled system of equations is partitioned into a mechanical phase at constant temperature, followed by a thermal phase at fixed configuration. The evolution of the internal variables is enforced in both phases. As shown in references 12 and 13 the isothermal split does not preserve the contractivity property

(b.i) Thermal phase. Using a BE scheme the discrete weak form of the energy balance equation and updated internal variables in the thermal phase take the form:

$$\begin{aligned} \frac{1}{\Delta t}\langle\, C_{sn+1}\,(\Theta_{n+1}-\Theta_n)+L_{n+1}-L_n,\zeta_0\rangle - \langle \boldsymbol{q}_{n+1},\nabla[\zeta_0]\rangle = \\ \langle R_{n+1}+(\tilde{\mathcal{D}}_{int})_{n+1},\zeta_0\rangle - \langle \bar{q}_{n+1},\zeta_0\rangle_{\Gamma_q} - \langle \tilde{q}_{n+1},\zeta_0\rangle_{\Gamma_{tc}} \\ \tilde{\boldsymbol{G}}_{n+1} = \boldsymbol{G}_n + \Delta\tilde{\boldsymbol{G}}_{n+1} \end{aligned} \tag{29}$$

(b.ii) Mechanical phase. Using a BE time stepping algorithm, the discrete weak form of the momentum balance equation and updated internal variables $\boldsymbol{G}$ in the mechanical phase take the form:

$$\begin{aligned} \langle \boldsymbol{\sigma}_{n+1},\nabla[\boldsymbol{\eta}_0]\rangle = \langle \boldsymbol{B},\boldsymbol{\eta}_0\rangle + \langle \bar{\boldsymbol{t}}_{n+1},\boldsymbol{\eta}_0\rangle_{\Gamma_\sigma} + \langle \boldsymbol{t}_{n+1},\boldsymbol{\eta}_0\rangle_{\Gamma_{mc}} \\ \boldsymbol{G}_{n+1} = \boldsymbol{G}_n + \Delta\boldsymbol{G}_{n+1} \end{aligned} \tag{30}$$

Results obtained with Scheme (b) are not the same as those obtained with Scheme (a), but the difference between them is of the order of the size of the time step, $\mathcal{O}(\Delta t)$, which is the order of the error of this type of operator splits. Note that in Scheme (b) the update of the internal variables $\tilde{\boldsymbol{G}}_{n+1}$ during the thermal phase is only necessary for the evaluation of the term $(\tilde{\mathcal{D}}_{int})_{n+1}$. In the simulation of solidification processes this term is usually negligible, and therefore this first update of the internal variables can be avoided. This is equivalent to performing an explicit update of the form $(\tilde{\mathcal{D}}_{int})_{n+1} = (\mathcal{D}_{int})_n$ and it results in an evident saving in computational cost.

4 NUMERICAL SIMULATIONS

The formulation presented in the previous Sections is demonstrated in the following selected numerical simulations. First, an assessment of the constitutive model is presented to establish qualitatively its validity. Then test industrial applications are presented and compared with available experimental data. Finally, a large size industrial analysis is performed and selected numerical results are shown.

The computations are performed with the finite element code COMET (COupled MEchanical and Thermal analysis) developed by the authors. In all the following numerical simulations the Newton-Raphson method, combined with a line search optimization technique, was used to solve the nonlinear equations arising from the spatial and temporal discretization of the weak form of the momemtum and energy balance equations. Convergence of the incremental (in time) – iterative procedure was monitored by requiring a tolerance of 0.1% in the residual based error norm.

assumed for the steel mould. Geometrical and material data can be found in the above reference. A gap dependent convection-radiation coefficient between the aluminium and the steel mould has been assumed.

Spatial discretization of the casting cylinder and the mould has been done using a finite element mesh consisting of 848 axisymmetric 3-noded triangles. Numerical simulation was done up to 90 s. of the solidification test using a time step of 1 s.

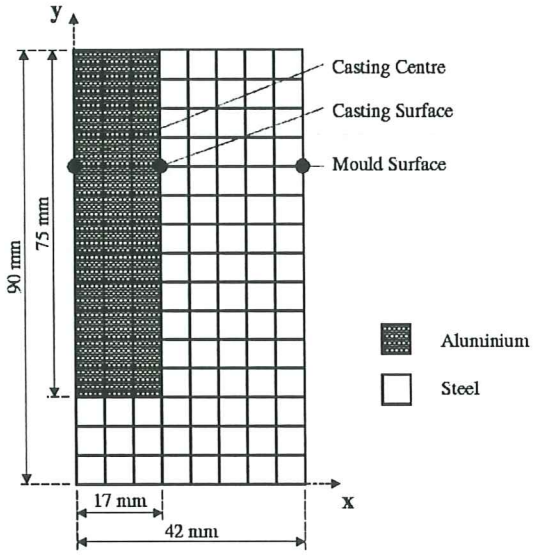

Figure 3. Cylindrical aluminium solidification test. Geometry.

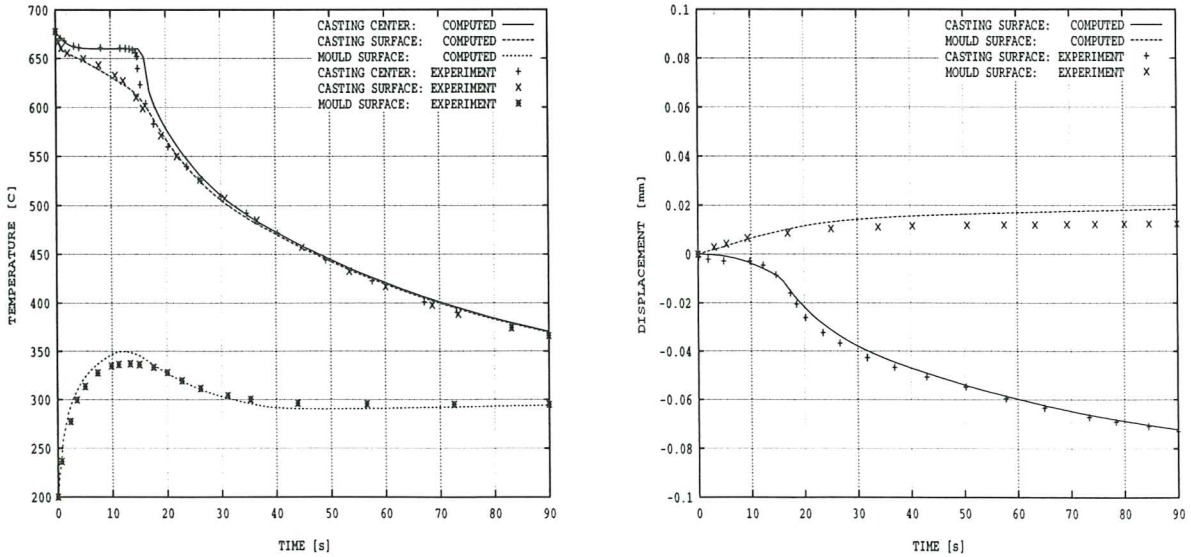

Figure 4. Cylindrical aluminium solidification test. (a) Temperature evolution at the casting center, casting surface and mould surface. (b) Radial displacement evolution at the casting and mould surfaces.

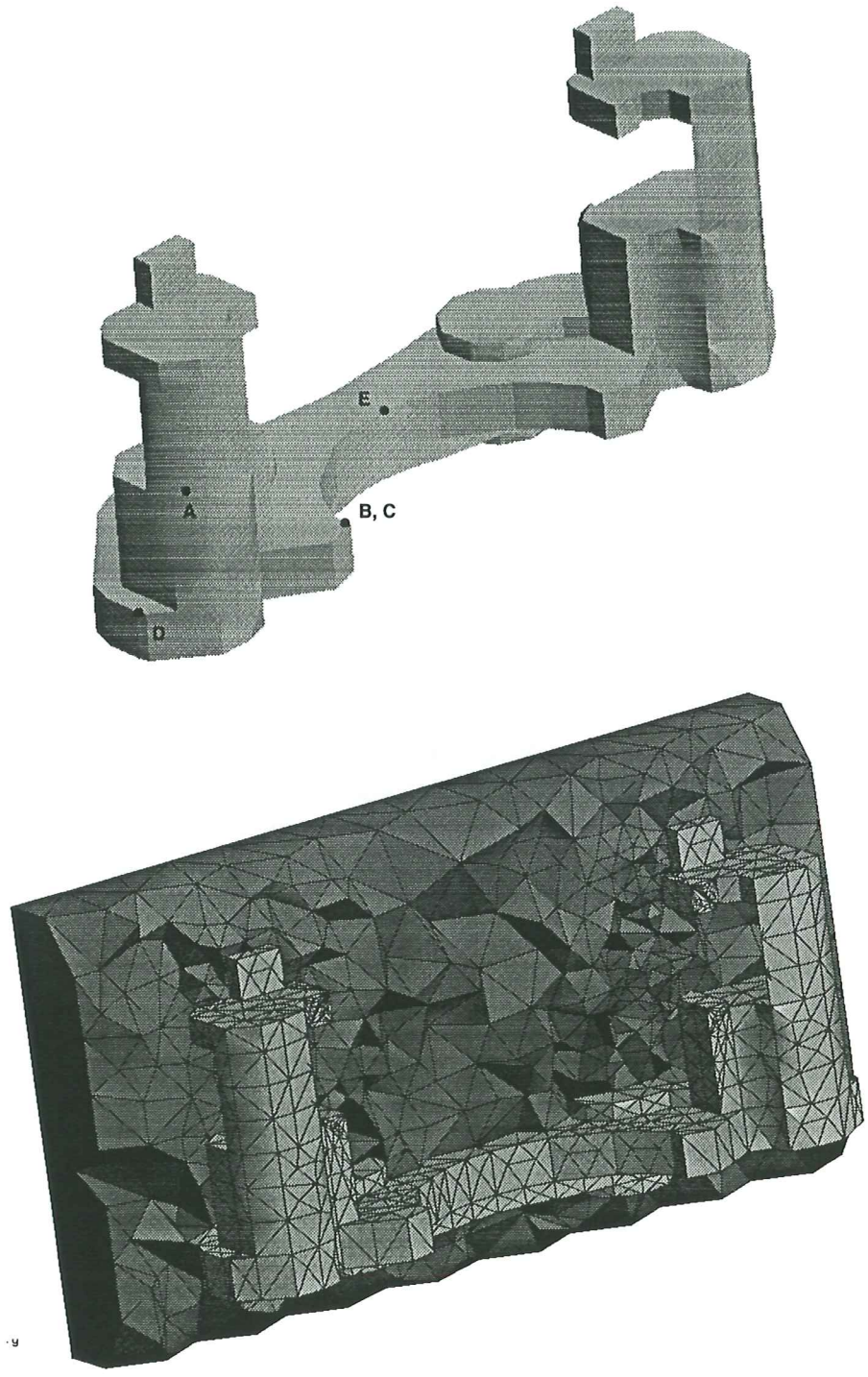

Figure 5. Solidification of a brake component. Geometry and finite element mesh.

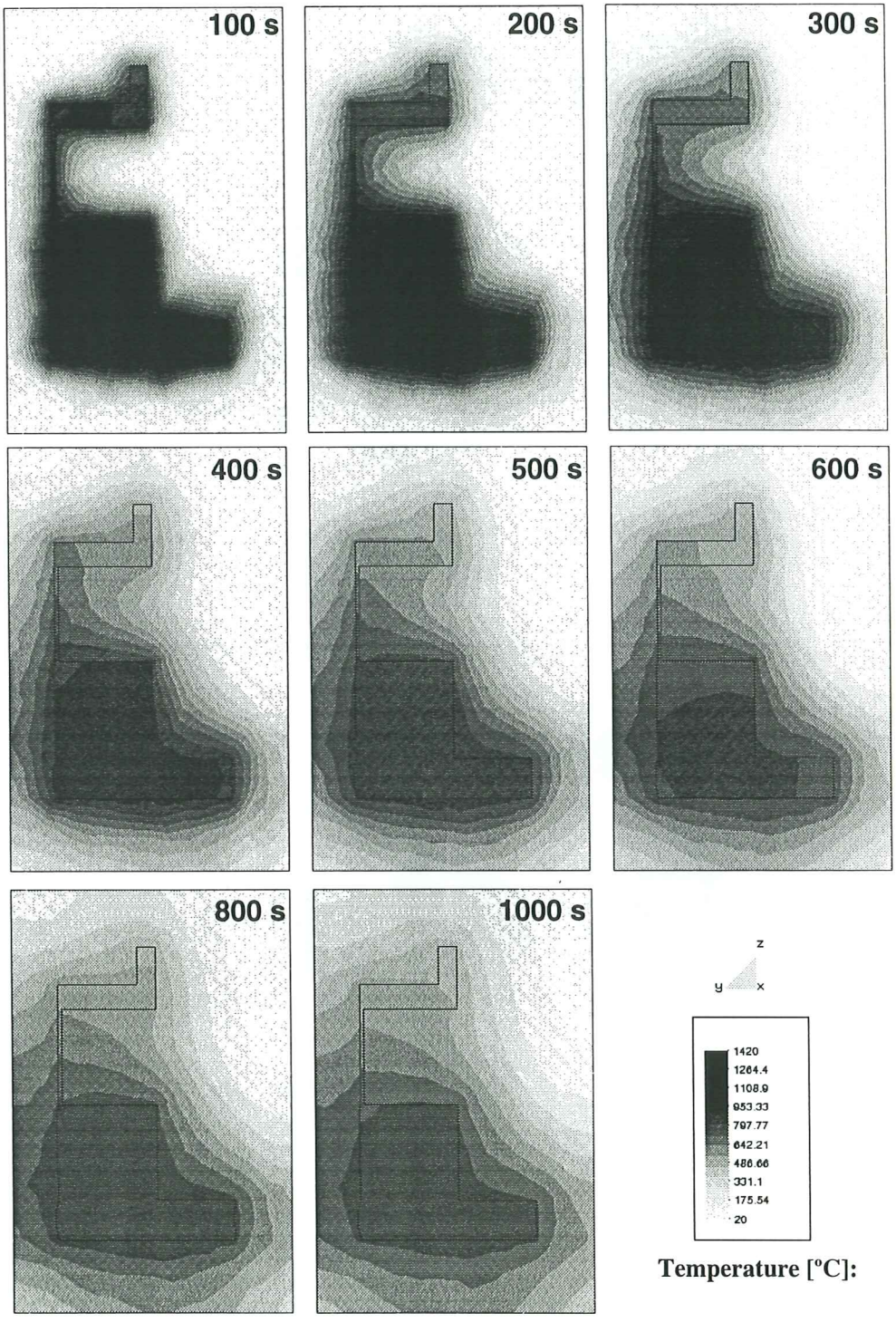

Figure 7. Solidification of a brake component. Temperature evolution on section y-z.

REFERENCES

1. B. D. Coleman, 'Thermodynamics with Internal Variables', *J. of Chemistry and Physics*, **47**, 597-613 (1967).
2. C. Agelet de Saracibar, M. Cervera and M. Chiumenti, 'On the formulation of Coupled Thermoplastic Problems with Phase-change', *Int. J. Plasticity*, to be published.
3. M. Chiumenti, *Constitutive Modelling and Numerical Analysis of Thermo-Mechanical Phase-Change Systems*, Ph. D. Thesis, Technical University of Catalonia, 1998.
4. C. Agelet de Saracibar, 'A new Frictional Time Integration Algorithm for Multi–Body Large Slip Frictional Contact Problems', *Comp. Meth. in App. Mech. and Engng.*, **142**, 303-334 (1997).
5. C. Agelet de Saracibar, 'Numerical Analysis of Coupled Thermomechanical Problems. Computational Model and Applications', *Arch. of Comp. Meth. in Engng.*, to be published.
6. S. Song and M. M. Yovanovich, 'Explicit relative contact pressure expression: dependence upon surface roughness parameters and Vickers microhardness coefficients', *AIAA*, Paper 87-0152 (1987).
7. P. Wriggers and C. Miehe, Recent Advances in the Simulation of Thermomecanical Contact Processes, in D. R. J. Owen *et al.* (eds.), *Proc. of III Int. Conf. on Computational Plasticity*, 325-347, Pineridge Press, Swansea, 1992.
8. G. Zavarise, P. Wriggers, E. Stein and B. A. Schrefler, 'A Numerical Model for Thermomecanical Contact Based on Microscopic Interface Law', *Mechanics Research Communications.*, **19**, 173-182 (1992).
9. R. S. Ransing and R. W. Lewis, A Thermo-Elasto-Visco-Plastic Analysis for Determining Air Gap and Interfacial Heat Transfer Coupled with the Lewis-Ransing Correlation for Optimal Feeding Design, in B. G. Thomas and C. Beckermann (eds.), *Proc. of VIII Int. Conf. on Casting, Welding and Advanced Solidification Processes*, 731-738, The Minerals, Metals & Materials Society, San Diego, 1992.
10. T. A. Laursen and J. C. Simo, 'A Continuum-Based Finite Element Formulation for the Implicit Solution of Multi-Body, Large Deformation Frictional Contact Problems', *Int. J. Num. Meth. in Engng.*, **36**, 3451-3485 (1993).
11. M. Cervera, R. Codina and M. Galindo, 'On the computational efficiency and implementation of block iterative algoritms for nonlinear coupled problems', *Engng. Computations*, **13**, 4-30 (1996).
12. F. Armero and J. C. Simo, 'A new Unconditionally Stable Fractional Step Method for Nonlinear Coupled Thermomechanical Problems', *Int. J. Num. Meth. in Engng.*, **35**, 737-766 (1992).
13. F. Armero and J. C. Simo, 'A Priori Stability Estimates and Unconditionally Stable Product Algorithms for Nonlinear Coupled Thermoplasticity', *Int. J. Plasticity*, **9**, 749-782 (1993).
14. D. Celentano, S. Oller and E. Oñate, 'A Coupled Thermomechanical Model for the Solidification of Cast Metals', *Int. J. Solids Struct.*, **33**, 647-673 (1996).